SI APPENDIX

SUPPLEMENTARY METHODS

Culture and irradiation conditions

Wild-type *P. tricornutum* (*Pt*1 8.6; CCMP2561) cells and transgenic lines were grown in f/2 Guillard media (1). For experiments in different photoperiods, cultures were pre-adapted to the different L:D cycles for 2 weeks before starting the experiment. For L:D experiments, cells were illuminated at 40 µmol photons m^{-2} s^{-1} of white light (Philips TL-D De Luxe Pro 950) either for 16 or 12 hours. For gene expression experiments in continuous darkness and continuous light, cells were pre-adapted in 16L:8D photocycles for 2 weeks, then transferred to D:D or L:L at the start of the experiment. For fluorescence measurement and growth analysis experiments in free running L:L conditions, cells were grown in 16L:8D cycles, then transferred to 15 µmol photons m^{-2} s^{-1} of blue light from ZT12 onwards. Cell concentrations were measured using a MACSQuant Analyser flow cytometer (Miltenyi Biotec, Germany) by counting the cells based on the R1-A (630 nm excitation, 670-700 nm emission) versus the R1-H parameters. Growth rates (μ) were calculated during the exponential phase of growth over four days. Cellular fluorescence rhythmicity assays were carried out by measuring the flow cytometer FL3-A parameter (488 nm excitation, 655-730 nm emission).

Analysis of the rhythmic processes

For the analysis of rhythmic parameters, each FL3-A fluorescence dataset was amplitude and baseline detrended, then normalized to the maximum value. For graphical representations, data were aligned to the mean values. Fitted curves of the average FL3-A fluorescence were calculated using the lowess fit function in R (span = 0.35). Circadian period, amplitudes and phases were calculated by Fast Fourier nonlinear least square algorithm (FFT-NLLS), evaluated within a period range of 20 and 30 h using the Biodare2 tool (biodare2.ed.ac.uk, (2)). This analysis allows to formally identify differences in rhythm profiles using the Relative Amplitude Errors (RAE) as a reliable proxy for rhythmic coherence. The RAE is a measure of goodness-of-fit to a theoretical sine wave. RAE is defined as the ratio of the amplitude error to the most probable derived amplitude magnitude. The RAE value ranges from 0.0 to 1.0, with 0.0 meaning a rhythmic component has an infinite precision and with 1.0 meaning the rhythm is not significant (error exceeds the most probable amplitude magnitude) (3). For L:L analyses, periods, phases and amplitudes were estimated starting from 33 h after the last dark/light transition. To evaluate if cell lines presented altered rhythmic traits, the obtained periods and

www.pnas.org/cgi/doi/10.1073/pnas.1819660116

phases were plotted against the RAE (Table S3 and Fig. S9) so to provide a measure of how well the observed outcomes are replicated by the fitted cos waves, as previously described (4). Eight to nine independent biological replicates were considered for the analysis in 16L:8D conditions (Table S2), while fifteen biological replicates where considered for the analysis in L:L conditions (Table S3). Three periods of oscillations were considered for each replicate in all period estimation analyses. Two-tailed t-test was used to determine statistical differences between mean phases, amplitudes, periods and RAEs (Fig 3, Fig. S8, Table S2 & S3).

RNA extraction and transcript analyses

For qRT-PCR analysis, *RPS* and *TBP* were used as reference genes. Each independent replicate of the qRT-PCR data was normalized against the maximum expression value of each gene (*i.e.,* gene expression range lies between 0 and 1 across the time series). Average expression and standard error were then calculated and plotted. The full list of oligonucleotides used in this work can be found in Table S5. For the nCounter analysis, gene specific probes (Table S1) were designed and screened against the *P. tricornutum* annotated transcript database (JGI, genome version 2, Phatr2) for potential cross-hybridization. Total RNA extracts (100 ng) from three biological replicates were used for hybridization. Transcript levels were measured using the nCounter analysis system (Nanostring Technologies) at the UCL Nanostring Facility (London, UK) and at the Institut Curie technical platform (Paris, France) as previously described (5). Expression values were first normalized against the internal spike-in controls, then against the geometric mean of the reference genes *RPS* and *TBP*. The 12L:12D and 16L:8D experiments of Fig. 1 were analysed by qPCR, while L:L and D:D experiments were analysed by nCounter. All sequence data in this publication have been deposited in National Center for Biotechnology Information Gene Expression Omnibus (6).

Immunoblot analysis

Proteins were extracted as previously described (7). Membranes were blocked with PBS-T 5% milk and incubated overnight at 4° C with α-HA (Covance) (1:2000) antibody and an α-D2 (1:10000) antibody used as loading control. Following incubation with HRP-conjugated 521 secondary antibodies (Promega), proteins were detected with Clarity reagents (Bio-Rad) and imaged with a G:Box camera (Syngene, UK).

bHLH1a subcellular localization

bHLH1a protein sequence was scanned using two online tools for subcellular localization prediction: ELSpred (8) and DeepLoc (9). For microscopic analysis, chlorophyll autofluorescence and YFP fluorescence were excited at 510 nm and detected at 650–741 nm and 529–562 nm respectively. Hoechst 33342 (Life Technologies) was used at a final concentration of 5µg/ml to stain nuclear DNA and stained cells were visualized by illumination at 405 nm and detection at 424–462 nm.

Generation of the *bHLH1a* transgenic lines

The full length *bHLH1a* coding sequence was obtained by PCR amplification with the specific oligonucleotides *Pt*bHLH1a-DraI-Fw and *Pt*bHLH1a-XhoI-Rv on cDNA template using the Phusion high fidelity DNA polymerase (Thermo Fisher, USA). The PCR fragment was inserted into the pENTR1A vector (Invitrogen, USA) using the DraI/XhoI restriction sites, and recombined with the pDEST-C-HA vector or the pDEST-C-YFP vector (10) both driving expression of the transgenes under the control of the *Light harvesting complex protein family F2* promoter (*Lhcf2p*). Transgenic lines were generated as in (11). Transformed cells were tested for the presence of the transgene by PCR and qRT-PCR analysis (see Table S5 for oligonucleotide sequences).

Selection of rhythmic transcripts and clustering analysis

For the selection of genes with rhythmic expression in the light-dark cycle, we used microarray data from (12). First, we identified all the genes belonging to the TFs, photoreceptors, cell cycle and metabolism-related categories (pigment synthesis and photosynthesis). Then, transcripts were ranked based on a defined t-value for each time point (mean gene expression of the replicate/(1+s.d.)) and those showing t-value >+0.7 or <-0.7 across the time series, were retained. The nCounter expression data was normalized against the maximum expression value of each gene, in a similar way to qRT-PCR expression data. This normalization was applied to the 3 replicates independently and for each condition (L:D and D:D) with the average expression value used for the clustering analysis. Hierarchical clustering analysis was performed with MeV 4.9 (13) using Pearson correlation. Peak analysis was performed using the MFourfit curve-fitting method defining average expression phases for each cluster (https://biodare2.ed.ac.uk, (2)).

For the selection of rhythmic transcripts in D:D, expression values were normalized using *RPS, TBP* and *ACTIN12* as reference genes. The genes with the highest values of standard deviation from the average expression over the two time courses (16L:8D and D:D) were

selected. A threshold equal to 1 was set using the published *P. tricornutum* diurnal microarray dataset (12) as background. Gene expression profiles were further empirically examined and false positives eliminated.

Data mining, protein sequence and phylogenetic analysis

The *P. tricornutum* bHLH1a (Phatr3_J44962) protein sequence was used as the query for BlastP analyses on the JGI, NCBI and MMETSP public database (14). The Pfam database was also searched for proteins possessing both the HLH and PAS domains. The retrieved sequences were analyzed using the batch search tool on the CDD (Conserved Domain Database) NCBI server to retrieve proteins presenting at least one HLH and one PAS domain only. We identified 100 HLH-PAS proteins from 71 marine algal species which were aligned using MAFFT (15), along with 22 HLH-PAS proteins from relevant metazoan (*Homo sapiens*, *Mus musculus* and *Drosophila melanogaster*) and unicellular Opisthokonta (*Monosiga brevicollis* and *Capsaspora owczarzaki*). As previously reported (16), no bHLH-PAS proteins were identified in Archaeplastida organisms, with the exception of the Rhodophyta alga *Galdieria sulphuraria*. Preliminary phylogenies were produced with MEGA 7 (17) to eliminate ambiguously aligned sequences, refining the alignment to 107 sequences and a final length of 198 aa (<5% gap per position). The best amino acid model to fit the data was estimated with ProtTest 3.4.2 (18). Phylogenetic analyses were performed with RAxML (1000 bootstraps) and MrBayes 3.2.6 (2.5 million generations, 2 runs, 25% burn-in) on the CIPRESS gateway (19). The final tree was edited in Figure Tree 1.4 (http://tree.bio.ed.ac.uk/software/Figure_tree/). GenBank accession codes of the genes utilized in the bHLH-PAS phylogenetic analysis are reported in Table S4.

Cell cycle analysis

P. tricornutum Wt and transgenic cells were synchronized in the G1 phase with prolonged darkness for 40h. After re-illumination, the FL3-A parameter was measured in cultures on an hourly basis for 12h using a flow cytometer (Miltenyi Biotec, Germany). At the same time, samples were harvested for cell cycle analysis. Cells were pelleted by centrifugation (4000 rpm, 15 minutes, 4°C), fixed in 70% EtOH and stored in the dark at 4°C until processing. Fixed cells were then washed three times with PBS, stained with 4',6-diamidino-2-phenylindole (at a final concentration of 1 ng/ml) on ice for 30', then washed and resuspended in PBS. After staining, samples were immediately analyzed with a MACSQuant Analyser flow cytometer (Miltenyi Biotec, Germany). For each sample 30,000 cells were analysed and G1 and G2 proportions were inferred by calculating the 2c and 4c peak areas at 450 nm (V1-A channel) using the R

software. A peak calling method was applied to the resulting histogram, based on a 1st derivative approach (20). The locations of G1 and G2 peaks were first determined using G1 and G2 reference samples and then used to identify G1 and G2 cells in the experimental samples. The area under each peak was used as a proxy for the proportion of cells in each population.

Figure S1 – Annunziata et al.

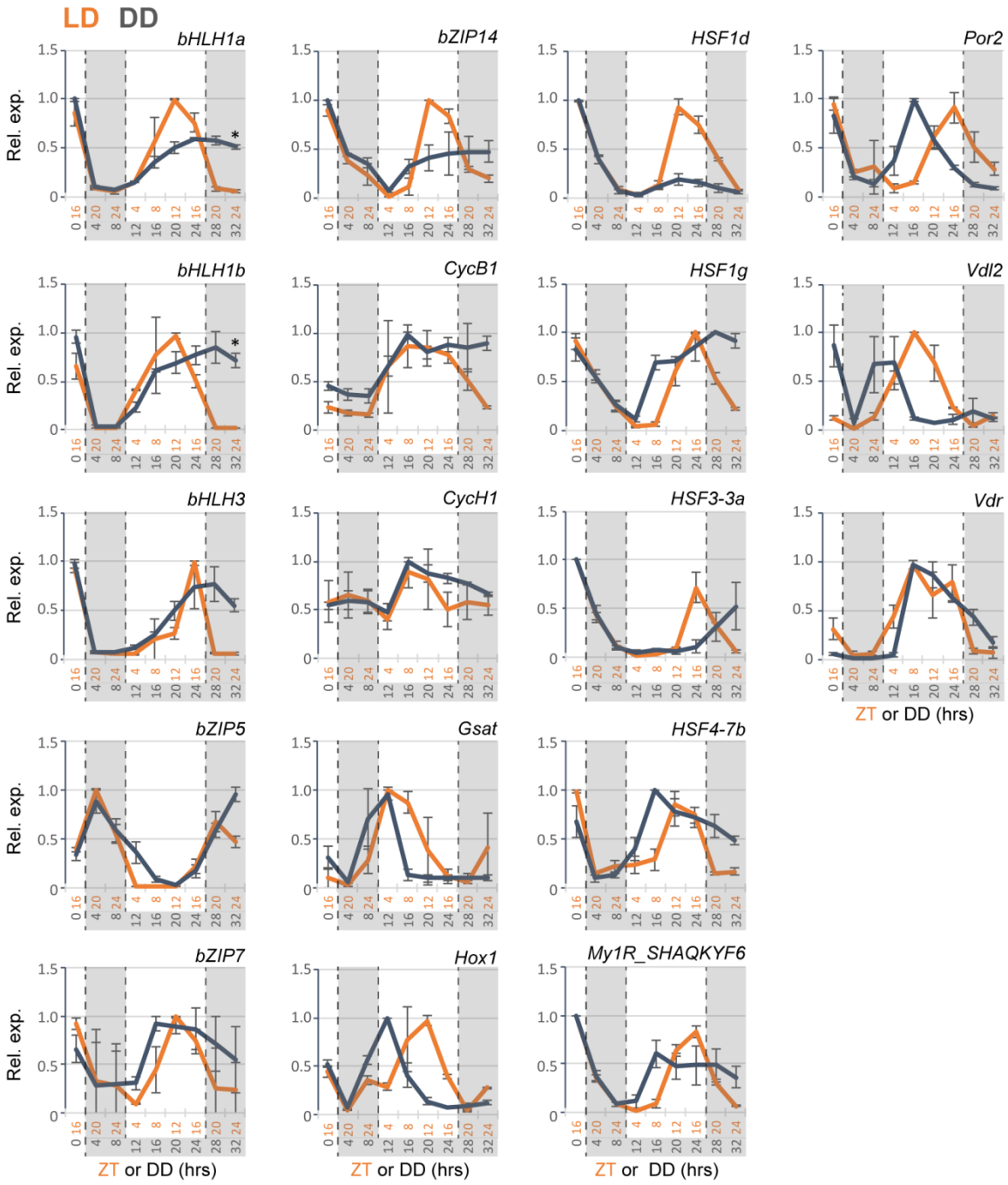

Fig. S1. nCounter expression analysis of genes maintaining rhythmic expression in D:D condition and 16L:8D condition in Wt cells. Data represent the average expression of biological triplicates ±SD and are normalized using the *RPS*, *TBP* and *ACTIN12* reference genes. Expression values are given relative to the maximum expression for each gene, where '1' represents the highest expression value of the time series. Results for cells grown in 16L:8D cycle are shown in orange (L:D); results for cells in constant darkness (following 16L:8D

adaptation) are shown in grey (D:D). For the *bHLH1a* and *bHLH1b* profiles in D:D, the asterisks on the last time points indicate that the expression at DD32 is significantly decreased with respect to the peak of expression of each gene (DD24 for *bHLH1a* and DD28 for *bHLH1b*) (*P<0.05, t-test).

Figure S2 – Annunziata et al.

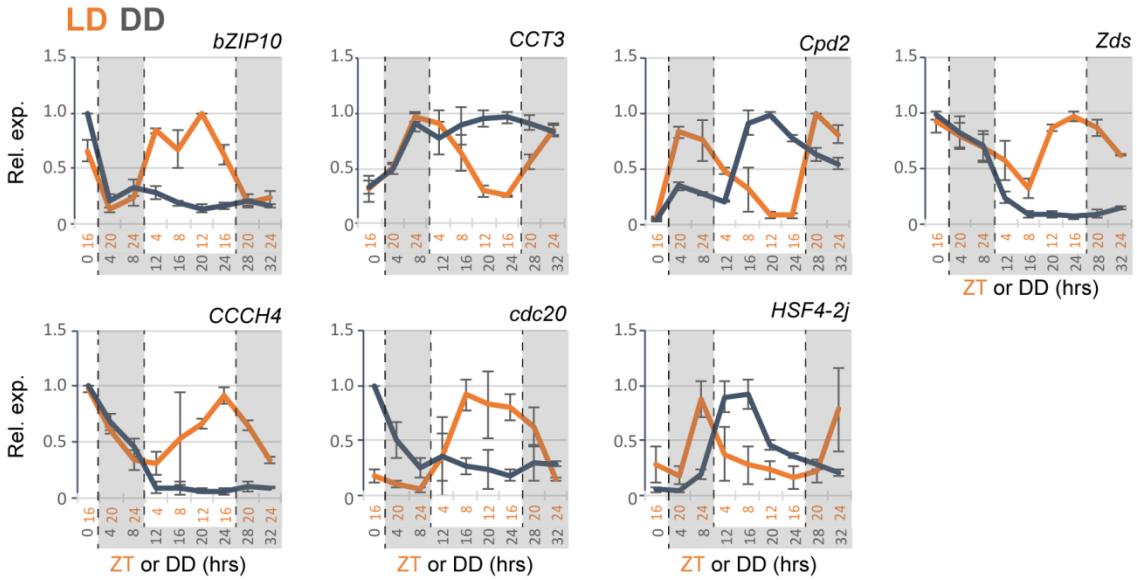

Fig. S2. nCounter expression analysis of representative genes with altered rhythmic expression in Wt cells in D:D condition compared to 16L:8D condition. Expression values represent the average of three biological triplicates ±SD and are normalized using the *RPS*, *TBP* and *ACTIN12* reference genes. Expression values are given relative to the maximum expression for each gene, where '1' represents the highest expression value of the time series. Results for cells grown in 16L:8D cycle are shown in orange (L:D); results for cells in constant darkness (following 16L:8D adaptation) are shown in grey (D:D).

Figure S3 – Annunziata et al.

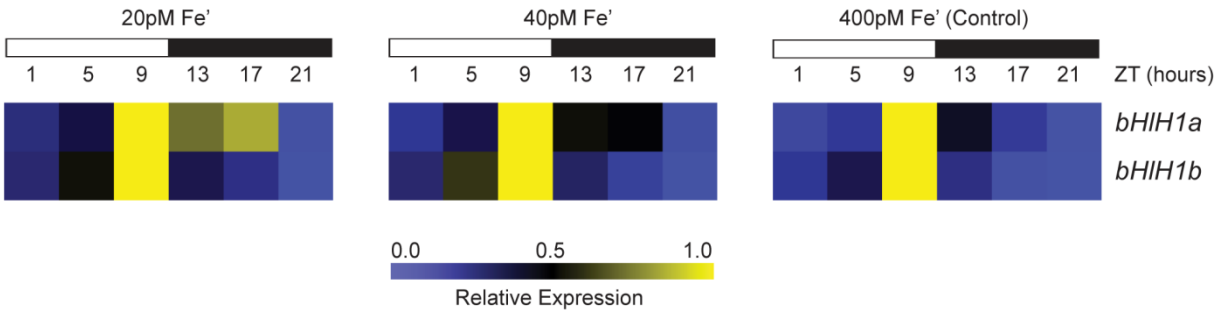

Fig. S3. Diel expression patterns of *bHLH1a* and *bHLH1b* genes under Fe-depletion conditions in 12L:12D photoperiods. Diel expression patterns of *bHLH1a* and *bHLH1b* in normal (400 pM Fe') and iron depletion conditions (40 and 20 pM Fe') were obtained using transcriptome data extracted from (21). Light and dark periods are represented by white and black rectangles. Expression values are given relative to the maximum expression for each gene, where '1' represents the highest expression value of the time series.

Figure S4 – Annunziata et al.

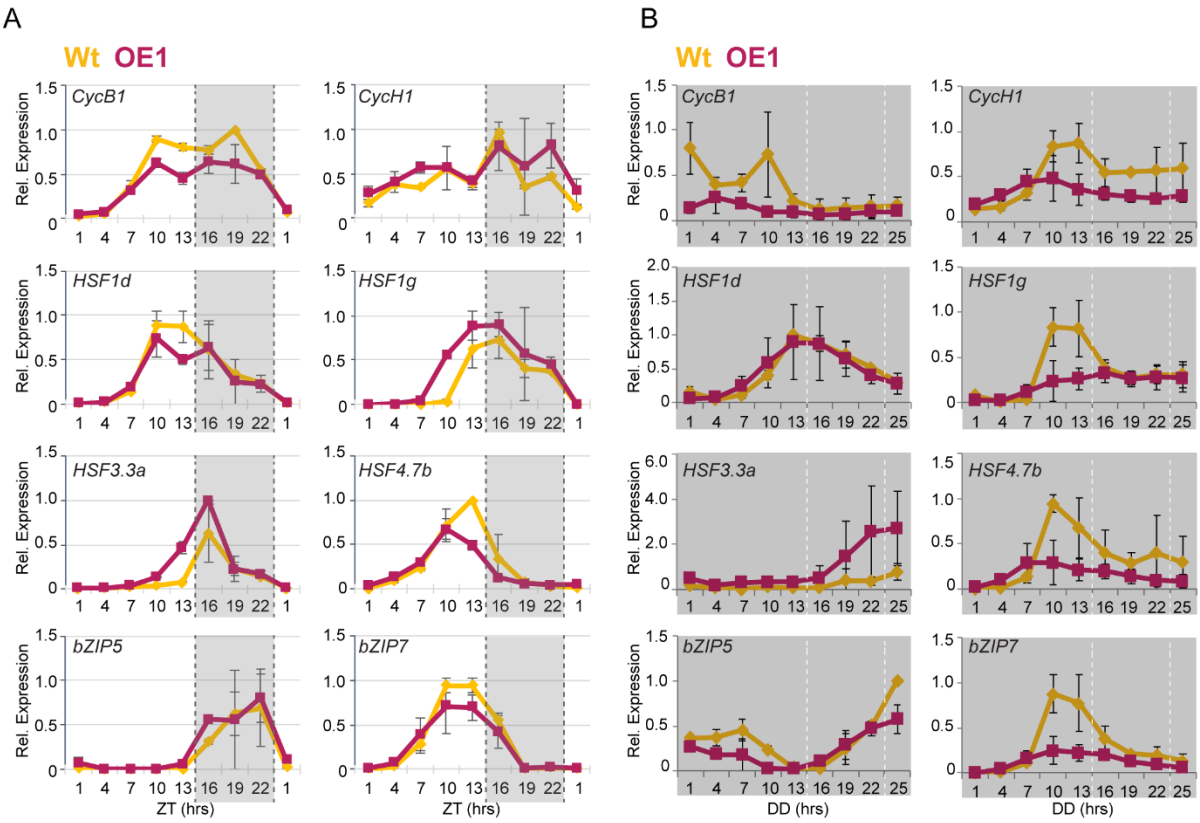

Fig. S4. Analysis of selected rhythmic gene expression profiles in L:D and D:D in Wt and bHLH1a OE1 cells. Cells were entrained in 16L:8D cycles, then kept in L:D or transferred to D:D and collected every 3 hours for 24 hours. Expression values represent the average of three biological replicates (n=3) ± s.e.m (black bars) and have been normalized using *RPS* and *TBP* genes. A: qRT-PCR analysis; B: nCounter analysis.

Figure S5 – Annunziata et al.

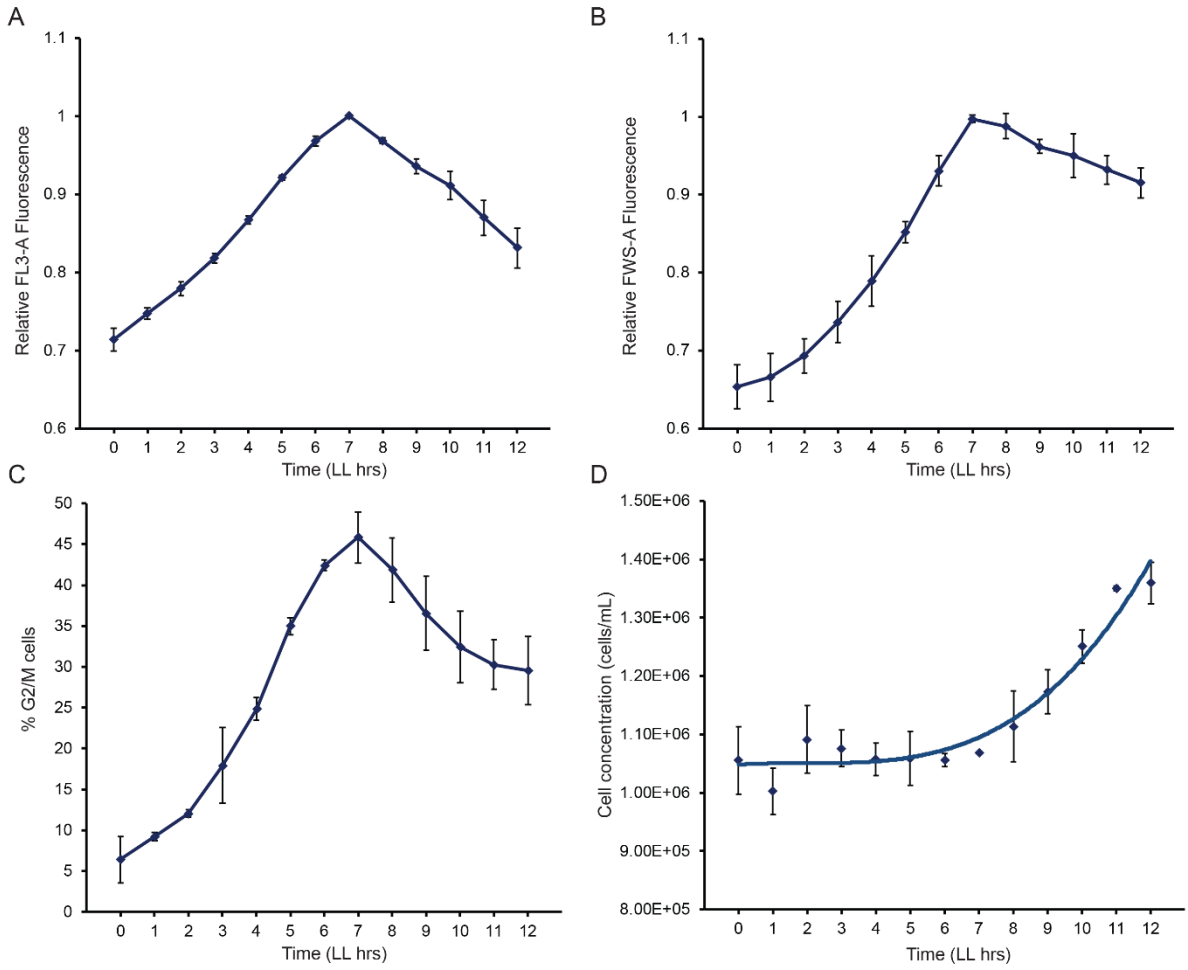

Fig. S5. Cell cycle progression dynamics of Wt *P. tricornutum*. A-B) Progression of chlorophyll fluorescence (FL3-A parameter) and cell size (FWS-A parameter) measured by flow cytometry each hour over 12h of illumination following dark synchronization. C) Proportion of cells in the G2 phase measured by flow cytometry each hour over 12h of illumination following dark synchronization. D) Hourly measures of cell density in re-illuminated cultures. The trend curve represents the third-degree polynomial regression. Results are representative of three biological replicates ± s.e.m (black bars).

Figure S6 – Annunziata et al.

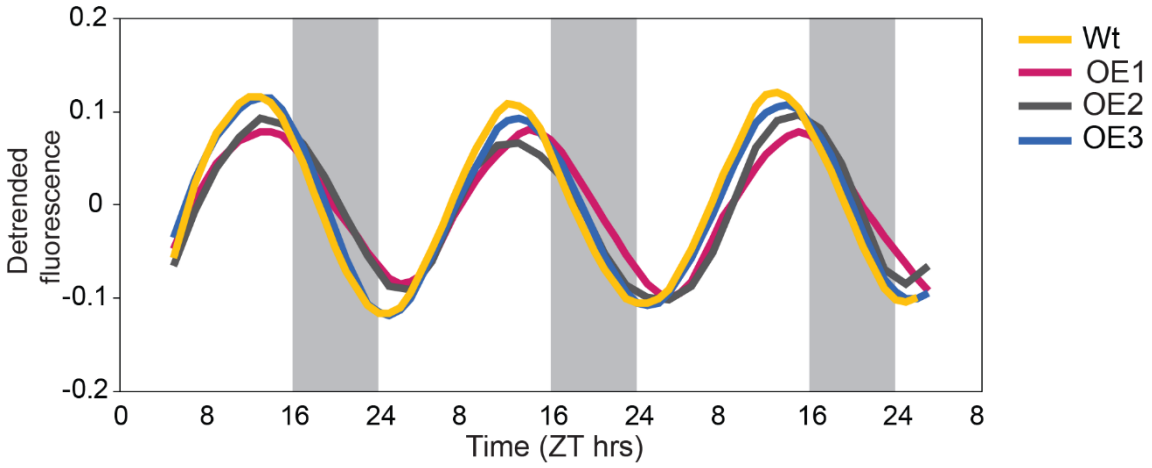

Fig. S6 Diurnal oscillations of chlorophyll fluorescence (FL3-A parameter) in Wt and bHLH1a OE lines. Lowess fitted curves of the mean FL3-A values in Wt and OE lines entrained under 16L:8D over 3 days ($n \geq 8$).

Figure S7 – Annunziata et al.

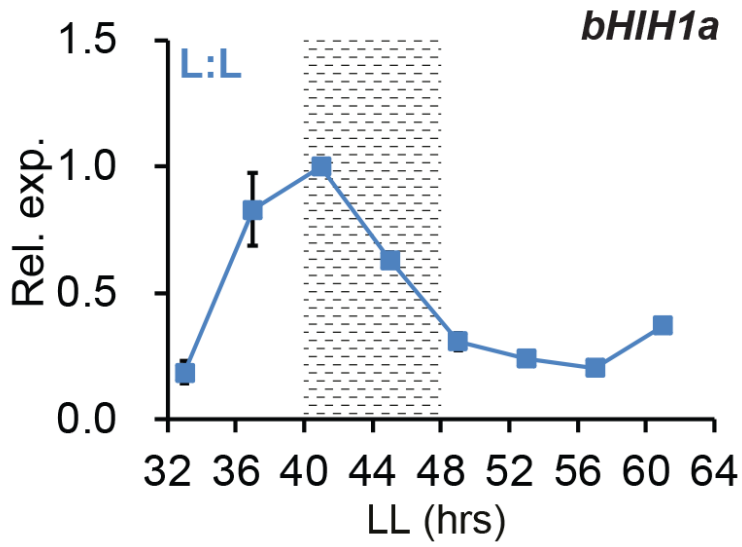

Fig. S7. Analysis of *bHLH1a* gene expression in continuous blue light. Cells were entrained in 16L:8D cycles, then transferred to constant blue light (L:L) and sampled every 4 hours for 28 hours. *bHLH1a* gene expression was analysed by qRT-PCR starting from L:L33. Expression values represent the average of two biological replicates (n=2) ± s.e.m (black bars) and have been normalized using *RPS* and *TBP* genes. Dotted region represents the subjective night in L:L.

Figure S8 – Annunziata et al.

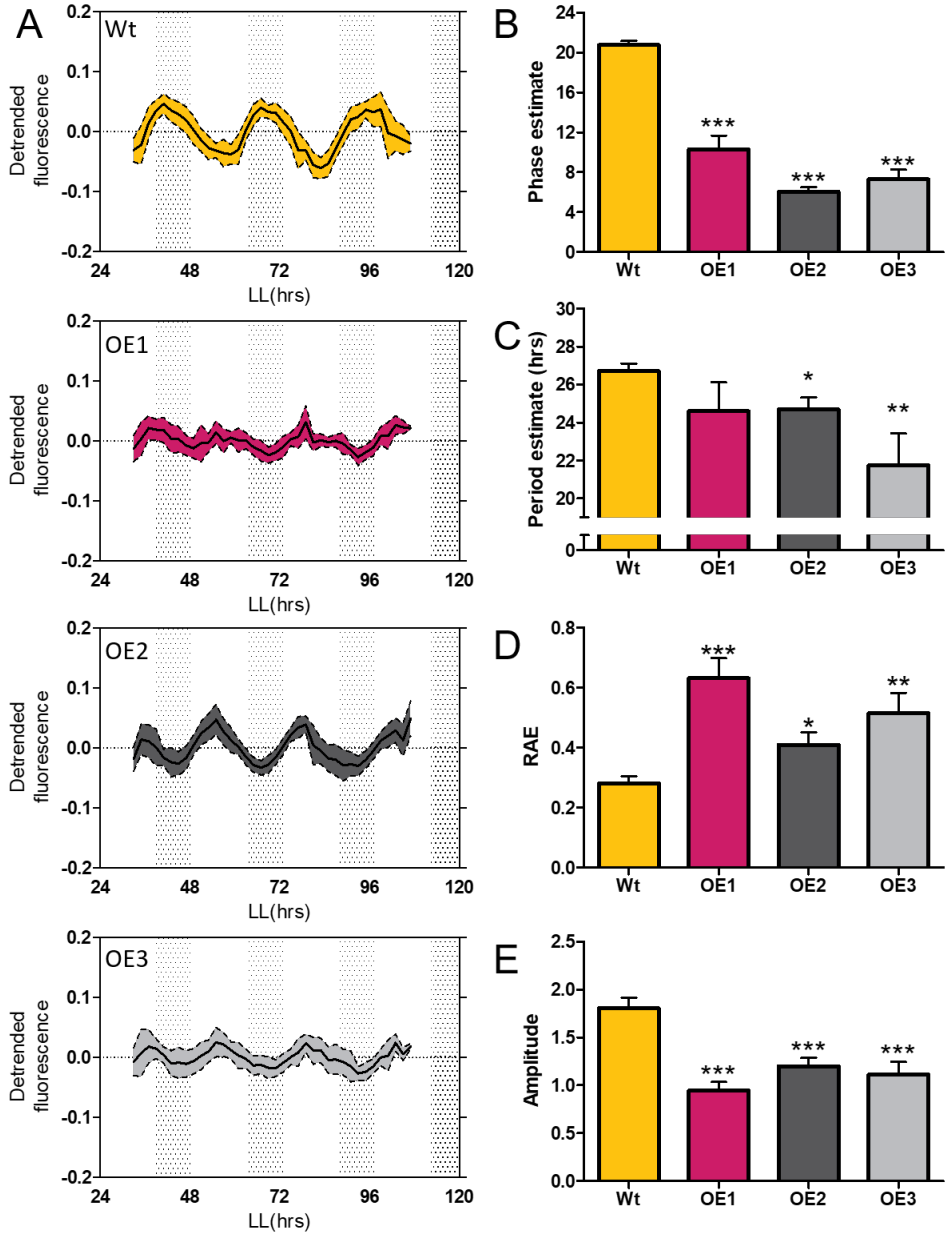

Fig. S8. Circadian oscillation of chlorophyll fluorescence in Wt and *bHLH1a* OE lines. A) Solid lines represent the average diurnal FL3-A fluorescence oscillation under continuous blue light (L:L) of Wt and OE lines replicates reported in Table S3 (n=15). Colored ribbons represent the standard deviation. B) Phase, C) period, D) relative amplitude error and E) amplitude of the FL3-A oscillations in Wt and OE lines (mean ± s.e.m., n=13 to 15, two tailed t-test between transgenic lines and *Wt*: *P<0.05, **P<0.01, ***P<0.001). The OE1 line also showed shorter average periods than the Wt, although it lacked a significant difference most likely due to the high variability introduced by the replicates with high relative amplitude error (RAE) (Table S3).

Figure S9– Annunziata et al.

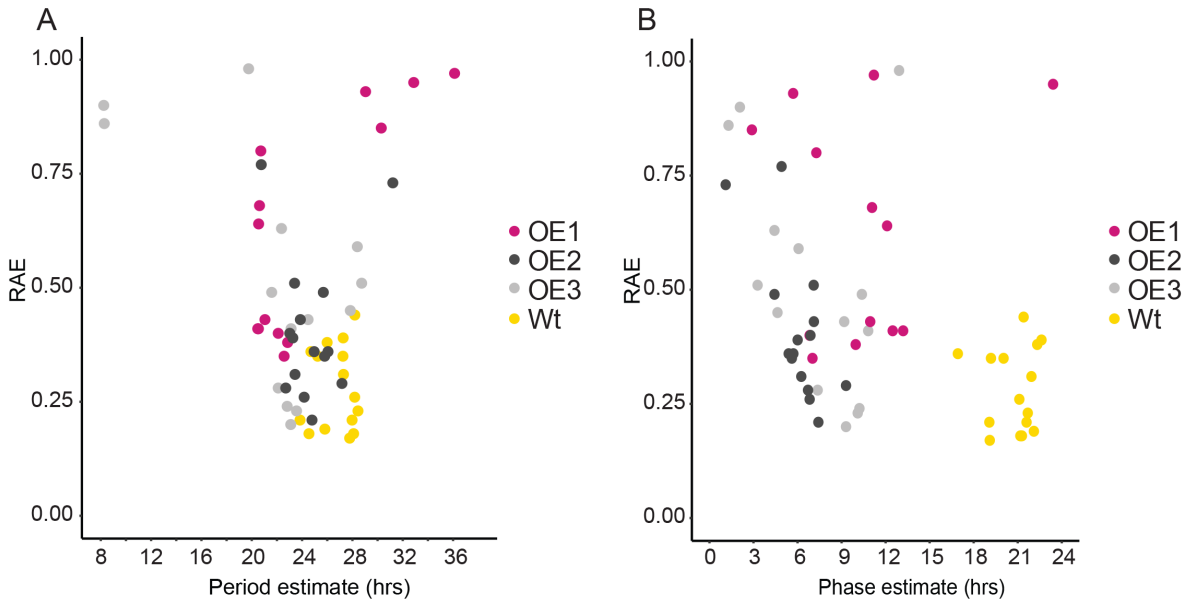

Fig. S9. Analysis of rhythmicity in Wt and *bHLH1a* OE lines under blue L:L. Relative amplitude error plotted against A) Period and B) Phase estimate for individual cell cultures growing in L:L (n=13 to 15, Table S3). Multiple dots of each color indicate independent replicate cultures.

Figure S10– Annunziata et al.

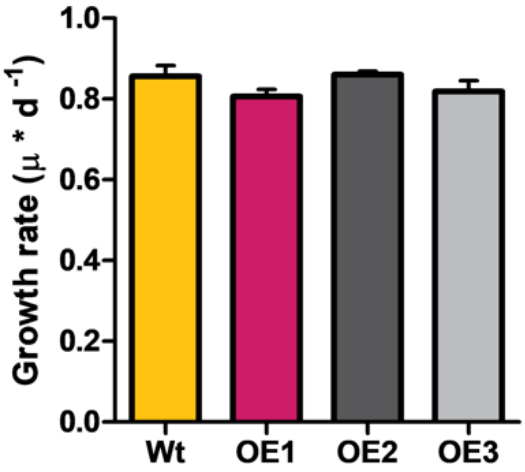

Fig. S10. Growth rate of Wt and *bHLH1a* OE lines grown in blue L:L. Cells were grown in 16L:8D conditions, then transferred to continuous blue light (L:L) and followed during five subjective days. Growth rates were calculated over four days. Results represent the average of three biological replicates ± s.e.m (black bars). *p* values were calculated by comparing Wt to the indicated OE lines via two tailed t-test. No significant difference among lines was detected.

Figure S11 – Annunziata et al.

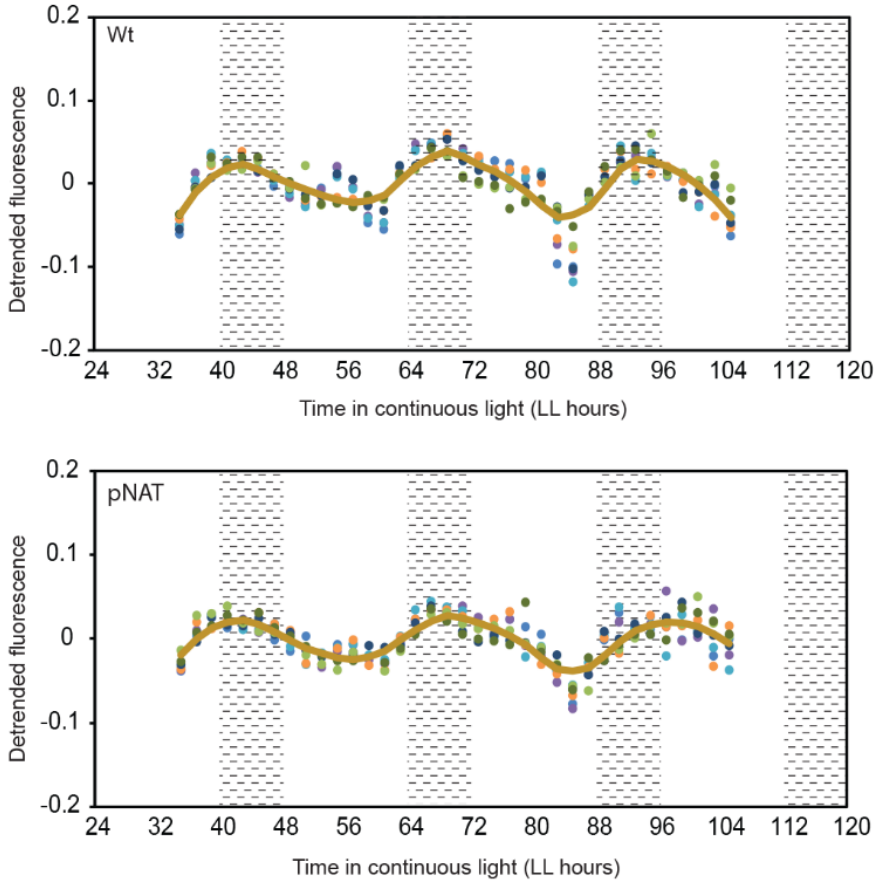

Fig. S11. Circadian oscillation of chlorophyll fluorescence in Wt and a transgenic control line (pNAT) under blue (L:L). Cells were grown in 16L:8D conditions, then transferred to continuous blue light (L:L) and followed during four subjective days (n=8). Colors in dots represent independent replicate cultures. White bars represent subjective days and dotted bars represent subjective nights. Brown lines in plots represent the fitted curves (lowess fit) of the average FL3-A fluorescence.

Table S1: Accession codes and sequence probes used in the nCounter analysis.

Category	Gene Name	NCBI Accession	Phatr3 Accession	nCounter Probe Target Sequence
Reference Gene	Actin12	XM_002182185.1	Phatr3_J29136	ATGTAAGCCTGCAGCCACTGAGGACTTGTGCTCGTAACCCTGATTTCGATATTCCAAAATGCGGCTCACTAAAAAGACATCGTAGTCCAGTGCCAGTCCC
Photoreceptor	Aureo1b	#N/A	Phatr3_J49458	TTATTGCCGAGTGCTGTACCTCGAGTCCGTTGTTTGAAGAAATGGACGGCATAGATCAAACGAAAGGGGCCAATCTGGAACGTGCCGATTTTTCATTGAT
Photoreceptor	Aureo2	XM_002183279.1	Phatr3_J15468	AGACGTTACTGTCACTCTCATGAACTACACTGCCGATGGTACACCATTTTGGAACAAGCTCTTTATTGCCGCATTGCGTGACGCGCAAAATAACATTGTC
TF	bHLH1a_PAS	XM_002179032.1	Phatr3_J44962	TACTTTGGTCAATATCAAAGTCAGTTTGGTACGAACAGCTCAGCATAGCCCTCGGTTTTTCAATGTGGCGTTGGTGCCATCAGACGATGCAGCGAAGCTG
TF	bHLH1b_PAS	XM_002178812.1	Phatr3_J44963	AGGAATTGACTACCGTGCTGTTTTCAATCATTGTCCATATGCCATGGGGGTGGCTTCATTGGACGGAAGAATACTGGTCTGCAACAGCTCTTTCGAATCT
TF	bHLH3	XM_002176560.1	Phatr3_J42586	ATCACTAGCGACACATTCAGATTCATCTGCGGGAGAAGGACGGTCTATTCCGTCAGTAGTTGGTACAAGTGTTAGCGGTTCAAGTCGCTCTGGGAACTGC
TF	bHLH5	XM_002177858.1	Phatr3_J43365	ACCCTCTTGCAGCGCAATCATTCGCTCCCGCATACGACTATGGGTCGATTTCTCAATGAACGCCATTCCTTTTCCTCAGACCTTTCGCTCTCGCTGGCGT
Cell cycle	BUB1/MAD3	XM_002178639.1	Phatr3_J10954	CGTGTGCTGCATGTATGCGGACAAAACCGATCGTCCACTGGAAGTTTTCCAGCATCTACATCAGCAAAGGATCGGGAGCGATATTGCCGTGTTCTGGATG
TF	bZIP10	XM_002177776.1	Phatr3_J43744	AAGCTGCTCGGGAATCGCGTCGGCGGAAGAAGGTTATGATTGAAGAACTTCAACGCAGCGTGATTTTCTTCTCGCGTGCCAACGGAACCCTCAAACAACA
TF	bZIP13	XM_002181635.1	Phatr3_J47278	CGCGGCGGCTTCGCGTGCTAAGATTCGATGCCGCATCACCGAACTTGAAACCGAGGTTAGTGGTTGGAAGGATAAATACACACAAGCAATGGAACGCTTG
TF	bZIP14	XM_002179477.1	Phatr3_EG02108	ATGCAGAGCTTGGAGGGTCGAGCTACGGATCTCAAGCATGAGCAAATTCGTTTAAAACAGATCATTAACGAAAAGAACACGGCGAACATTCTGGTGGGGC
TF	bZIP16	XM_002181462.1	Phatr3_J47279	CTTTTGGAAGCAGTCACAAATCCGCAAACATGAACAGTTCCAACGCCCAGGAAGTCGCTCGTCAACTGAACGAAGATCCTGCGCTCGCTCGGAAGCGTCG
TF	bZIP18	XM_002176556.1	Phatr3_J42577	ACTCTTCTATAGCGGAATCCGAGGCCGATTTCAAAACTATAGCTCAGGCTGCTGTTTCGAATCTGATCATGTCGGCTGGAACTACCAAGGTTGAATCTGG
TF	bZIP19	XM_002183101.1	Phatr3_J48701	CCTGCACCTTCTCAAATCAGCTGTGCAACGAGTGCAACAAGAAGAAATATTGGCTGCCGAGGCATTACCTACACCTTTTATAGGCGTTTTGCGATTTGGC
TF	bZIP24	XM_002184633.1	Phatr3_J49887	TTGTCACGGGGCCAACAGACTATCTGGAAAGATCACTTCTTGCCCAAAGAGAAGCGGAAAGAACTCGTTCGGCTTTGTCAAGCATCGCGCTTCGGGGGAA
TF	bZIP25	XM_002185584.1	Phatr3_J46647	TCGTCGTTCACGATGGCATCTGTACCAACTCACCTAGTAGGAAATACTGTCATCACTGATACCAGTTATCAGCCAGTTTCGTCGCTATTACCTGCAGCGG
TF	bZIP26	XM_002182641.1	Phatr3_EG02494	GATTCTTTGACGGACTCAAGGAGCGACAACTTGTCATCGACATCTCAGGAGCTTTCGGTGCGACAGGAAAAGGTCGAAGCCGCTTTGAAATCGAAACCTC
TF	bZIP5_PAS	XM_002179145.1	Phatr3_J45142	CCCTTGTTTCCGAACAGCGCATTCGATCCGCAAAACAACGCTAGCAACAACGCACAATCACAGTCGCAAATGATGATGCAGAACGTGGCTATTATGAGTG
TF	bZIP6_PAS	XM_002184884.1	Phatr3_J50039	CGCGCAATCTAATACACAATATCAGCTAGACAGCCCACAACATCCCGAAAATACGATGTCGCAGTGTAGACCGCAGCAGGGTTCAAATAATTCGGCGAAC
TF	bZIP7_PAS	XM_002183297.1	Phatr3_J48800	CGTGAGAGACCTTGCCATGCGTAATCAAGGATTAGAGGCATTAGCGGCGATTGCGACAGCAAGCTCGTCTTCAGGGCACACGTTTAGTACCAACACGAAT
Metabolism	CaThioredoxin	XM_002184396.1	Phatr3_J49634	CTGGAGAGCCCTACCGTGCTAGTGTCCGTGTATTGGAAAAATGTCGTTGTTTTGCGTTCAGCGTAGAAGACATTCCTGACAGCTCCATTCTGAGTCTGAA
TF	CCCH4	XM_002181104.1	Phatr3_J13664	CATGTGCCGCCTTGGAGCGTCGCACATTAACATGTCTACTGGCGAAAACATTCGAAAGGACATTGATGGTCCGAAGCCCAAGCCAATCTTAAATACTCTA
TF	CCCH8	XM_002186091.1	Phatr3_J44042	TCCGAAAAATATGTGCGAAGAGTCCCACTTGTCGCGTATGTTCTTGGCTCATACGAGTATTGCGCCGACGGAAGTGGAAGAGATTGAGTTTGCGGGTGAA
TF	CCHH1_CCCH20	XM_002179821.1	Phatr3_EG02317	TAACTACAACAACGTTCCTCAGCTAAACGGTTTGAACCATCTGCCTTCTAAGAACCTATCCGACTTACATTCCCACTATCAAGATCATAGGAGTCCAAAC
TF	CCHH14	#N/A	Phatr3_J34600	GCCCAGTTTCTGCGGAGGCATCCCGTTCAATCCGCCGATCTGAGTTACGAAACGCACTACATGGCGTACCAAAAAGTTTACACTGATGCCCGAGTTGTTC
TF	CCT3	XM_002185983.1	Phatr3_J43850	AAACGCTGCCGCCGCGTTTGGAATAAGAAGATTCGCTACGGTTGCCGTAAAAATTTAGCAGACCGCCGGTTGCGCGTGAAGGGGCGATTCGTGAAACGTT
TF	CCT4	XM_002178133.1	Phatr3_J44285	TATGAATGCAGTCGACCGGGAATTGAGTTTCCATCAAACAACAGAGCTAAGCTGGTCGAGCACCAGCACGGCCTTTCGCCCATTCCTTTTCACGATAGTG
Cell cycle	cdc20	XM_002180546.1	Phatr3_J12783	TTACGACGGAATTGCTTTGAAGAAAATCAGAACACTTCATGGGCACACAGGCCGAATATCGTCGTTGGGATGGAACCAACACTGGTTGAGTTCAGGCGCA
Photoreceptor	Cpd2	XM_002179343.1	Phatr3_J54342	TCTGGTGTGCGGCAATACGGCGGACAGTGTTTCGGAGCTCTGTAAAATTGCTTCTGAGATTGGCGCGAGTGCAGTCTATTGGAATCGCGAGATGACACCT
Photoreceptor	Cpd3	XM_002180035.1	Phatr3_J51952	CTCTGATTTTTCTCCGATACGCGAATACCGTCAATGGATGGAACTCCAGGCCGTACCTATCTTGGAGGAAGCGAAGGTCCCGTTTTATCAGGTTGATGCC
Photoreceptor	Cpf1	XM_002180059.1	Phatr3_J27429	GGATGCGTGCCAAAAATCCGAATCACTCCTTCCGATTTACGTAGTCGACCCTGAATTTCCCTTCGCGCAAACTGCTGGGTGCCGCGCCGGTACAATTCGT
Photoreceptor	Cpf4	XM_002184521.1	Phatr3_J55091	CTCGATCCCTTGTTGCGGCGCAAACGAGACTGCATTTCCGTAATGGGTCTACCTAATGATTTTGTAGACTCCATTGTCGAGGCAGCGTTTGAAGCAGCTG
Photoreceptor	CryP-like	XM_002178853.1	Phatr3_J34592	CACTTTATGGTGGCGAAACAGCCGGACTCGCACGATTGTTTGAAGGATTACTTCGAAACGCGCAACGGGATGCTGGGGCCGAACTATTCGACCAAATTCA
TF	CSF2	XM_002185522.1	Phatr3_J41601	GAACAGAACGAAAAGATTCGGGACGCTTATGCATTCCAACAGACGAAAATCGACGAGGCTCATCAACTTATTGTCAATTTGGGCATGGACGTTGCAGACT
Cell cycle	CYCB1	XM_002180361.1	Phatr3_J46095	TTAGAGAAAAGTCAATCGCAAATCCTGAGCTCCGAGCGGTGAATAAAAAGTACAGCGGTCATCGATACGGCGGAGTTGCTTCGACCGTTCTGGTATTTGA
Cell cycle	CYCH1	XM_002185709.1	Phatr3_J36892	TTTGCGATGGCTCGCGTTTGACGTTTCGGTTTCCCATCCGCACCGAGGAGTTGCCGCAATCGTCAACCATCTCGTGGATTGCTCACCTCAATGGTTTGGC
Photoreceptor	Dph	XM_002179026.1	Phatr3_J54330	CAACAATTCCATTACAACCAAAGAGCTGACGGAATGTGATCGTGAGCCTGTGCACTTGATCGCAAACGTACAAGGGGGTACCGGCCATTTGTTGTTCATT
Cell cycle	dsCYC2	XM_002179247.1	Phatr3_J34956	GATATTGCCGTTACCGAACGCGAAATAATGACTGCTCTTTCCTGGCACTTGCATCCTCCAACCGCTATTGGCTTTTCACGAATGTACTGGTCTCTGCTGG
TF	E2F_Dp2b	XM_002181452.1	Phatr3_EG02016	TGATTTGAATAGAGCTGTGCAGGAAATGAGGGTACAAAAGCGCCGGATTTATGACATTACCAACGTTTTGGAAGGTATTGGGCTGATTACCAAGGATAGC
Cell cycle	E2F1	XM_002176842.1	Phatr3_J43065	GTGTGGGTCTCATCGAAAAACGATCCAAAAACACAGTCGCTTGGAAAGGGAGTGAGCTTCTTCTTGGCTCGTCCTTTTCAAGTGCCGCCAAGCAGAGAAT
Cell cycle	FtsZ	XM_002185088.1	Phatr3_J42361	GAAAAAGGAGAATGAAGCAAGCGATTGCCGCGATTGAGAGGTTGCGAGAGAATGTGGATACGGTCATCGTAGTGTCCAACGACAGACTGCTCGAGATTAT
Metabolism	GapC1	XM_002182255.1	Phatr3_J22122	TGAAGGGATTCCTCGGATACTCCGACGAACCGTTGGTCTCCACCGACTTTGAAGGTGACTTGCGCTCCTCCATCTTTGATGCCGATGCCGGTATCATGCT

Metabolism	Gsat	XM_002180931.1	Phatr3_J36347	ATTCGTTTGGTCCGCGCACACACGGGTCGGGAAAAGGTCATCAAGTTCGAAGGATGCTACCACGGACACGCCGATTCATTTTTGGTCCAAGCCGGATCCG
TF	Hox1	XM_002184935.1	Phatr3_EG02213	AACAAACATCGGTTCACATACTGCGTCATACCGGACAAGTCCCGACAGTCGAAGATGTTACGATCCTTACCAATGTTCCGGCGGAACGCATTCTCCGAAC
TF	HSF1.3b	XM_002179894.1	Phatr3_J35419	CTCCAGGGAACAACTCGATACCAGAGTTCCTCTATCAGCTAACAAAGATGCTGACGGATAACAACCGAGATATTATTGAATGGACAAATGGCAAGATTGA
TF	HSF1a	XM_002177362.1	Phatr3_J43051	CCACCAACGTCGGATAGCTCCGACTGGGGTTCTCCAATCCAATCATCCAAGCCAGCTGTTGATCTCTTAACGAGGAGTATGCCGCAATGGACAAATATAC
TF	HSF1b	XM_002181395.1	Phatr3_J47181	TTGTAGTGGACACTTCGATGCTCGAAGAGGTCATCAACGAAACGCAGCCACTCGTTGGAGACAAAGGTAGCTTCTCCCTCTTGACAAATAGAGCACCAGT
TF	HSF1d	XM_002178673.1	Phatr3_J44750	GTCACCATTCCAGCATCGGATGCGGCTCCTTACGCCATTTCTCCCGAAACCTCACCGAGAGACTTGACTCTGAGACACAACGAAATTCCCAACCTTGATG
TF	HSF1g	XM_002177016.1	Phatr3_J42514	ATAGAGAATCTGCAAGCACTAGGGACCATGACGACTACTTCATCGAAGCGTAGCATTACAGAGAGCGAAGATAGTTCCCTGTCAGACTCAGCATCAGGAG
TF	HSF2.1a	XM_002181681.1	Phatr3_J47360	AGCCCTTGCCGCTGGAATTTTGGGCTCGTTGTCGCCTCAAGTCAACCAACCACAGCCGTGGATGATCCAACACGCCCTGTCAATCGCTCAAGCGTTAGTT
TF	HSF2.2c	XM_002185405.1	Phatr3_J50481	GGACTGGAAACTGTAAGCGCGACATATTTCCGCAGCGCCTTCTAGCGATTTTGAGCGAATCATCCCTATCTGACATTATCACTTGGCTTCCACATGGACG
TF	HSF3.2b	XM_002186124.1	Phatr3_J44099	TTGACTCCTCGCGACCAGCAAGCACTTAGCGCGTTTCAACAGTCCCTCGGTGCATCCGAGAGTCAGTTCAAGTCTATGAGCTTTTCCACCACAACTCCTC
TF	HSF3.2e	XM_002179404.1	Phatr3_J45206	TTGGAACGGGAACGCTTTCCCTCAGATTAGCAATCCGCAACCTTCGCCTACTCCTCCAAGTTCGACGATGGTAAATACTTCGGACTTAGCAAGACTACTT
TF	HSF3.3a	XM_002179738.1	Phatr3_J45393	TCTGGGCAAATCTTTCGTATGGAAGGTTTGGCGACGCCGAGTAGTCAGGGAGTTGGCGTAACCACAGGCAGTTTGCCGCTTCGAGACCAAGACGCTGTTA
TF	HSF3.3f	XM_002179735.1	Phatr3_J45389	CATGCCAATTGAACACCCAATTCAGCCATACATGGAAGAGCTTAAGAGGGTCCATCTTGCAGCGGCGGCGGGAAGTCTCGAAAATGCGCTTCGAATTTTG
TF	HSF4.2c	XM_002182762.1	Phatr3_J48361	CGCACGTATATCACGATTTCGCACAAGTGCGGCCCGACGCGGATCCCATGATGATCGTCCGGAAAAAGACTGGAGGAGTCACTCAGCCATTTCCCGAAAA
TF	HSF4.2j	XM_002177548.1	Phatr3_J43363	GTCGGCGGACGGGCCTTTATCATTCACAAGCCTGACAAGTTCTTTAAGGATATAGTGCCGCTATATTTTCGCCAGTCGCGGCTGAGTTCATTCAAGCGGC
TF	HSF4.3a	XM_002184368.1	Phatr3_J49594	CGCGAACACTCGCGTTCCAATGTCGCGGAAGAACCTTCCAAGCGAACCTTTGTTCAGCATATTTACCATGACCATATGAACGACCCTGAGCAGGTGGATG
TF	HSF4.3b	XM_002183012.1	Phatr3_J48558	CTGTCTTGAGCCTATCGCAGCAGTGGCGCCGAATTTCTACGCTATGCCAACTACTGAAGGTGGAGACAAAGACCAATTATTCTCGATCCAAAATACGTGG
TF	HSF4.3c	XM_002183081.1	Phatr3_J48667	AAACTGTCAGTCATGCTTGACCATGTAAAAGCCGCAGGATTGGACGACGTTATTTCTTGGGCCAGTCATGGCCGCTGTTTTAGCATTCACAACCCAGACC
TF	HSF4.4b	XM_002184371.1	Phatr3_J55070	CCCATTCCGGTAAACCCGGTTTCCAACTTGGGCGTATCCAGAGCGCCTAGTTTTGGTAAGCTCGAACCAGGCCAATTCGCTGCTTATGGCGGTTGTATGA
TF	HSF4.6a	XM_002184347.1	Phatr3_J49557	CTCAAACACTGGCGATTGCCGTATCGCCTCGTTCCGCCATCCAGTGCACGCCAACATCGTGAATCCTTCGCACTTTCGCTCTGTCTCCAATAACGGGCAC
TF	HSF4.7a	XM_002185271.1	Phatr3_EG00092	CGGACATCCCGGGGCGGATTTGAGATCGACGCGATAGTGTCATTCTTGCGTTCCAAGAGTATTTCGCAACTCTACATTATCGGTGGTGACGGTACTCACC
TF	HSF4.7b	XM_002184277.1	Phatr3_J49596	CTCGAGGTGGTGTGGGAACTCCTTTTCCACTCAAGCTGCACGAAATGCTTCAAAATGTCGTACAAGACGGCTACGCTCACATTGTATCGTGGCAGCCTCA
Metabolism	Lhcx1	XM_002179724.1	Phatr3_J27278	AATCCTTGAGAATCTTCAGGGTTAAAGAGTGCATCCATCCAAAACTGGAGGTATGGCTGGTCACATGCACAGAGTTAACAACCAATCCCTTTTCAAGCGA
TF	Myb1R_SHAQKYF4	XM_002178425.1	Phatr3_J44331	CGTATCTGCCGAATCGGTCTCTGGTGCAAATCAAGTCCCACGCCCAAAAAGTGCTCAAGCGCATCGATCAAGGCGAACACGTCTTCCGACGTATCGAGGA
TF	Myb1R_SHAQKYF5	XM_002181623.1	Phatr3_J47256	ACGCTTCACCTGGCCCGAAGACTTACACCGGGATTTTGTATCGGCAATTTTTGATGTCGGCTTGAAACAGTCGTCACCGTCCACCATTTTGGAAACCATG
TF	Myb1R_SHAQKYF6	XM_002180835.1	Phatr3_J46535	TAACGACGAAGCGCAAATCCTTACCGACAAACTTGCCGTCCCGCAAAAAGGGTAAGACACGAAAGTCTGCCGCCTTGGTACAGCGTAATACTTCAGTTTC
TF	Myb1R10	XM_002181361.1	Phatr3_J37257	CATATCCCTCTTCGGGGCCCTCACTTCCCTGTACAAGTGAATCTTTGGGGGTGAAAGCGAATCGTAGAAAGAAACGTGCTAAGGACGAGACCTCGGTTCT
TF	Myb1R4	XM_002181410.1	Phatr3_J47205	AAAGTTCGTTGCAGGTTTAGACGGAACGTCTACCGCATTGTCAATGGGAACAATCCGGCGAGTAGGATTCACCCATATGCGATTGAACTTCTGGAAGCCG
TF	Myb2R3a	XM_002181911.1	Phatr3_J47726	TCCATCTTTCCTTTGAGCGACTGTGACGACCTGTGGAGGGAGAGTGATTTTTGTCACTGTGAAGTTGTCGGTACTCCGGCACTCGGCAGGTAAAATACTC
TF	Myb2R3b	XM_002182076.1	Phatr3_EG02275	GCGCACAACGGTTTAAAGTGATTCGGGATTCATTCACAACAGTCAATGGCTAATTGGCCTCCATCGTTCACTGGTTGACATTTGCGATCGGCCCAACACT
TF	Myb3R1	XM_002182738.1	Phatr3_J15016	GTATGATCCTGGAGTGTCATTTGACGTTGGGAAACCGCTGGGCCGAAATTGCCAAGCGTCTACCGGGAAGAACTGATAACGCTATTAAAAATCACTGGAA
TF	Myb3R2	XM_002180449.1	Phatr3_J6839	CGAATTCTCATAGGAGCACAGGACACAATGGGAAATCGATGGGCTGAGATTGCCAAGCGGCTGCCAGGACGTACGGACAATGCGATAAAGAATCGCTGGA
TF	Myb3R4	XM_002180741.1	Phatr3_J36337	GACAGATGCCGAAGACGCAATTGTAATGGATGCGGTCAATTCCAGCTCGGAGCAACCATTTACTCGTTGGTCAGACTTGGCGCAACGTCTACCCGGACGT
TF	Myb3R5	XM_002184658.1	Phatr3_J7959	GACGTCGTTATCTGAATTGCTTGGACCCAACAATCCGAAAAGACGAATGGACGGAGCAAGAGAAAGAAGCTTTGTTTGATGCACAGCGGCGCATGGGAAA
TF	Myb5R	XM_002185245.1	Phatr3_J50365	TCAACACCACATAAACGCTCGTTTCAGGCTTTGGATGTGTTAGTGAACGCGGTTGGTTTTCATCGAGAACCAAATGACCAAATGAAGCAGACGAAGATGT
Cell cycle	PCNA	XM_002182225.1	Phatr3_J29196	AATGCAGGAACCGGTCGAACTCACCTTTGCCCTGCGCTACCTCAACTTTTTTACCAAGGCGACTCCGTTGAGTGGACACGTCATTATCTCCATGGCACCG
Metabolism	Pds1	XM_002180135.1	Phatr3_J35509	AGCATGGCCAAGGCACTCGATTTCATTGATCCCGACAAATTGAGTATGACGGTCGTTTTGACCGCCATGAATCGCTTTTTGAACGAAGACAACGGCCTCC
Metabolism	petA	GI:118411009	#N/A	TCTCTGGATCAGGAGCCATAACAGGGAAAATTAACTCTTGATGAGTCTTTCCTGCAATTGGTCCAACTACTAAGATATTATCAAATTCACTACTATACGG
Metabolism	Pgr5	XM_002178672.1	Phatr3_J44748	GTAACGTTCGCGCTTCTGATCGCTACCGCTGCCGCGTTTCGCGTGGCGGGCGGAGCCACCGGGGGTTCTTCCTTTGTGCTTTCCCGACGAACCAGCATCG
Metabolism	PgrL	XM_002177043.1	Phatr3_J42543	CCACAACAAGTAGCGTTTCCAATTTAGACAAGACTACGAACAAACGATGCGAGTCAACTCTGTGGTATTTGGCCTTTTGGTGTTCTCGGCCGTCAGCGAT
Metabolism	Por1	XM_002179653.1	Phatr3_J12155	TCGGGTGGTGAGATTTTTGAGAATCAGCAGTCCGACGCAGTACGGGATCTTCCTACCGCCAAGAAAATGTGGAAACTGAGTAGGGAAGCAGTTGGTCTTT
Metabolism	Por2	XM_002180956.1	Phatr3_J13001	AATCACCACTATTCCGTGAAAAGCGCCCGTGGTTCCGTAAATACTTTCCCATCTTTATGAAGTTTATTACGGGAGGATACGTTGGAGAGCACGAAGCCGG
Metabolism	Por3	XM_002177432.1	Phatr3_J43164	CGCGTTCTCAACACGAGGAAAAGCGGTGAGACTCATGATTCGTGATCCGACCAGTAGTCGTATCGAGGCACACCGTAGCGTGGGAGACGTAGACGTTCCC
Metabolism	psaA	GI:118410964	#N/A	GCTAAGAAGAACGCCCAAGTAGTTCCAATACCACCCAATAAATAATGAGCTAAACCAACTGCACGACCCTGAGTAATGCTTAATGCACGAGGTTGGATTG
Metabolism	psaD	GI:118410999	#N/A	TTAAATGTACGTAATTGGGTTCCCAATGCTAAACATTGCTCTTTGCGCGCTAAGTATAATAAATTTTCTCCACTACGCATGATAGCTGCTCCACCAATTG

Metabolism	psbC	HQ912250.1	#N/A	GGCCCAACAGGTCCTGAGGCTTCACAAGCACAAGCATTCACGTTTTTAGTTCGAGATCAACGTTTAGGTGCTAATGTTTCATCAGCACAGGGTCCAACTG
Metabolism	Psy1	XM_002178740.1	Phatr3_EG02349	ACCTGTCGTCGTGGGAATTGCGATTGGAGCGTTTGTGGCAATACGGACAAGTACAGGATGTCTTTGACCTGTGCTTGCTAGATCTTCGAATCCAGTATCC
Reference Gene	Rps	XM_002178225.1	Phatr3_J10847	CTCCGCGCATTTTTGCCCGGTTCCCATTTGACCGGACAGTTGCCCGACGAAGATCTCATTGGAAACAACTTGCAGCTTAAATTCCTCGAAGTCAACCAGG
TF	Sigma70.1a	XM_002182291.1	Phatr3_J14599	GACAATTAGGGGTATCTCGGGATCGGATTCGCCTTGTCGAAACCCGAGCACTGAACAAATTGCGACACCCGCAACAAAATTACAAGCTGCAGTCTTACGT
TF	Sigma70.1b	XM_002182124.1	Phatr3_J3388	TTCTTGGTCATTGGAAGAAACGGCCAAACAACTAGGGATGTCTCGGGATCGGATTCGCCTTGTCGAAGCCCGAGCACTGAATAAATTGCGACGTCCACAA
TF	Sigma70.2	XM_002178682.1	Phatr3_J5537	ACGTGGATTGCGATTCGCCACCTACGCCACTTACTGGGTCACCAATTCCGTACGCTTCTGCTTCCAAACCGCATCCACCGGATGTTTGCGGGTACCGGTA
TF	Sigma70.3	XM_002185461.1	Phatr3_J17029	TATGATGGTTCCTGATCTAAAGAAGCAAATTCGTCGCTCGCTTCGCGCCAAGGCTGCCCTGACGGAATCAAATATTCGACTCGTGGTATCCATTGCGAAA
TF	Sigma70.4	XM_002177232.1	Phatr3_J9312	AACCCGAAAGATCTCGGTCACGAAAGTCACGATTTGCTAGGGGACACAATCTCCGCCAGTAGTGCTCTTTTTGACGAAAGCACACCCGAAAAACGAGTCG
TF	Sigma70.5	XM_002182854.1	Phatr3_J14908	AAGAACTCATACAGGAAGGCAGTTTGGGATTGTTGCGCGCGGCCGAATTGTTTGATCCCGAGCGAGGACTGCGATTCAGCACTTACGCGGTAGTGTGGAT
TF	Sigma70.6	XM_002178042.1	Phatr3_J9855	CTGGAAAAATCAATATGGAAGCTATTCGGCAGACCATTGAAGAAGGACTGGAAGCCAAAAATCAGCTAGTCACTTCGAATCTGCGGATGGTACAGAGTGT
TF	Sigma70.7	XM_002185047.1	Phatr3_J50183	AATGATGACGCTCCTCTCGCATACGGTGGAACTCCGTCGTATCAAGCAAATCGAAGCTGATCTTGCTTTGACGTATCCATCTTCCCGGAAACCCACTACT
TF	Taz2	XM_002178935.1	Phatr3_J44807	CCTAATGTAGAGACTGTAGTGGTAAAAGCGAAGCGCGCAGCCTCGACTATTTGGACTTTACTTCATGCACAGAATTGCGTTTTGGGGGACAGATGCCCAC
Reference Gene	Tbp	XM_002186285.1	Phatr3_J10199	CTGATTTTTTCCAGCGGTAAAATGTGCGTGACCGGAGTCAAGAGCACACACAACGCCAATCTGGCGGCGAAAAAGTTTGCCTACATTGTGGAGCGCGTCG
Metabolism	Vde	XM_002178607.1	Phatr3_J51703	GGCGATGACGGATCATATCCCGTTCCCGCACCCGAAATCGTCGTACCCAAGTTTGACACCAAGTTCTTCGATGGACGACTCTACATCTCAGCCGGACAAA
Metabolism	Vdl1	XM_002180599.1	Phatr3_J36048	AAGGCTCTCTTTAGCAATCCGCGTGGAATCAAAGGTGTCTCCTGTTTGGGACGCTGCAAGGGCGAGCAATCGTGTGCGACGCGGTGTTTTGCCGAATTCG
Metabolism	Vdl2	XM_002180015.1	Phatr3_J45846	ACACACCGCCTTCGGCAATGAATATCCAATTTCCGGAGCCAGACGAATCACTCCATGTCTGGGACCACGTACGAAACATCGGTAAAGTGTGTACCGGGTT
Metabolism	Vdr	XM_002177477.1	Phatr3_J43240	GTCGCTTGCGGTGCCAACGAAGCCTATGATAAGTTTCCTTCGCAGAACCAACTCTTCTATCCCGCTGCTCGCGGTCGAGATTTGTGGTACGATCCCGTTT
Metabolism	Zds	XM_002184417.1	Phatr3_J30514	CGGCGTCAACGAATCCATGCGGGACACCGCCAACGTACTCGCCCGTTTTAATTCACTCATTCTCGCCCGAGTCTTTGGACACGCCGACGTCACGGAACTC
Metabolism	Zep1	XM_002179586.1	Phatr3_J45485	TTCCCAATGAAGTTTTCTACCACGGTGTCATCGGCACTGTTCCTGATCGCGTCGGTATCGACCACGACTTCCTTCACACCCGTCCAGTCCTTTGGCGTGC
Metabolism	Zep3	XM_002178331.1	Phatr3_J10970	CCAAGGTTTTGACCAAGATGCCCACCATGGATGTTACCGTACTGGAACAAACGTCCGAATTCAAACGGTTCGGTGGACCCATCCAGCTCGCTAGTAACGC

Table S2: Calculated periods, phases, amplitudes and relative amplitude errors of the Wt and bHLH1a OE lines growing in 16L:8D. P-values obtained via t- test between Wt and the OE lines are shown. Amp., amplitude; RAE, Relative Amplitude Error.

Data	Period	Period P value	Phase	Phase P value	Amp.	Amp. P value	RAE	RAE P value
Wt	23.9		13.44		0.1		0.15	
Wt	23.71		12.41		0.12		0.12	
Wt	23.86		11.95		0.13		0.13	
Wt	24.58		12.21		0.11		0.1	
Wt	25.71		10.32		0.12		0.21	
Wt	24.79		12.15		0.12		0.12	
Wt	24.24		12.81		0.15		0.19	
Wt	23.89		12.27		0.12		0.15	
Wt	23.64		12.89		0.11		0.19	
Wt average	24.26		12.27		0.12		0.15	
OE1	23.87		15.24		0.07		0.24	
OE1	24.53		16.17		0.07		0.23	
OE1	23.29		16.53		0.06		0.37	
OE1	23.18		18.16		0.07		0.52	
OE1	24.17		15.23		0.08		0.28	
OE1	24.67		12.19		0.14		0.09	
OE1	24.41		12.14		0.12		0.09	
OE1	23.77		13.32		0.09		0.16	
OE1	23.64		12.63		0.08		0.22	
OE1 average	23.95	0.2940	14.62	0.0078	0.09	0.0042	0.24	0.0653
OE2	23.65		15.47		0.11		0.19	
OE2	24.04		14.8		0.11		0.21	
OE2	24.23		14.78		0.11		0.22	
OE2	24.18		14.98		0.11		0.23	
OE2	23.34		14.22		0.09		0.21	
OE2	22.82		15.05		0.08		0.24	
OE2	21.91		14.14		0.08		0.32	
OE2	22.42		13.71		0.07		0.38	
OE2	23.6		12.24		0.08		0.33	
OE2 average	23.35	0.0206	14.38	0.0002	0.09	0.0021	0.26	0.0007
OE3	24.14		14.05		0.13		0.13	
OE3	24.49		13.73		0.12		0.18	
OE3	24.55		12.29		0.11		0.21	
OE3	24.31		11.32		0.1		0.25	
OE3	24.43		11.19		0.11		0.23	
OE3	23.74		11.96		0.11		0.17	
OE3	23.74		11.97		0.12		0.17	
OE3	24.77		12.31		0.11		0.21	
OE3 average	24.17	0.9607	12.58	0.8640	0.11	0.3037	0.20	0.0364

Table S3: Calculated periods, phases, amplitudes and relative amplitude errors of the Wt and bHLH1a OE lines growing in L:L. P-values obtained via t- test between Wt and the OE lines are shown. Amp., amplitude; RAE, Relative Amplitude Error.

Data	Period	Period P value	Phase	Phase P value	Amp.	Amp. P value	RAE	RAE P value
Wt	25.99		22.33		2.41		0.38	
Wt	25.24		20.04		1.68		0.35	
Wt	24.7		16.92		1.69		0.36	
Wt	25.81		22.1		2.43		0.19	
Wt	24.54		21.18		2.55		0.18	
Wt	23.83		19.07		2.14		0.21	
Wt	28.19		21.4		1.51		0.44	
Wt	27.27		22.62		1.59		0.39	
Wt	27.29		21.93		1.37		0.31	
Wt	28.1		21.28		1.88		0.18	
Wt	28.18		21.11		1.59		0.26	
Wt	27.25		19.18		1.21		0.35	
Wt	27.78		19.1		1.52		0.17	
Wt	27.97		21.6		1.4		0.21	
Wt	28.44		21.69		2.12		0.23	
Wt average	26.71		20.77		1.81		0.28	
OE1		FAILED Could not find cos waves that fit the data						
OE1	30.3		2.89		0.44		0.85	
OE1	29.04		5.7		0.46		0.93	
OE1	20.62		11.08		0.94		0.68	
OE1	20.72		7.28		1.12		0.8	
OE1	20.54		12.1		1.1		0.64	
OE1	20.48		12.48		1.55		0.41	
OE1	20.53		13.2		1.33		0.41	
OE1	21.05		10.95		1.09		0.43	
OE1	22.85		9.96		1.01		0.38	
OE1	22.57		7.02		1.04		0.35	
OE1	22.1		6.82		0.61		0.4	
OE1	36.12		11.2		0.72		0.97	
OE1		FAILED Could not find cos waves that fit the data						
OE1	32.87		23.41		0.86		0.95	
OE1 average	24.6	0.17	10.31	< 0,0001	0.94	< 0,0001	0.63	< 0.0001
OE2	27.17		9.3		0.99		0.29	
OE2	24.79		7.42		1.19		0.21	
OE2	24.17		6.82		1.14		0.26	
OE2	26.06		5.4		1.25		0.36	
OE2	23.86		7.11		1.17		0.43	
OE2	25.79		5.61		1.71		0.35	
OE2	23.02		6.88		1.23		0.4	
OE2	23.4		7.1		0.88		0.51	
OE2	24.96		5.71		1.41		0.36	
OE2	23.27		6.01		1.35		0.39	
OE2	22.7		6.71		1.74		0.28	
OE2	23.44		6.26		1.56		0.31	
OE2	25.69		4.43		1.02		0.49	
OE2	31.21		1.1		0.85		0.73	
OE2	20.75		4.91		0.54		0.77	
OE2 average	24.69	0.0108	6.05	< 0,0001	1.2	0.0002	0.41	0.0118
OE3	8.28		1.3		0.55		0.86	
OE3	8.23		2.07		0.46		0.9	
OE3	28.39		6.07		0.72		0.59	
OE3		FAILED Could not find cos waves that fit the data						
OE3	19.75		12.92		0.56		0.98	
OE3	24.48		9.18		1.73		0.43	
OE3	23.12		10.81		1.51		0.41	
OE3	22.1		7.37		2.15		0.28	
OE3	27.83		4.63		1.08		0.45	
OE3	28.74		3.28		1.2		0.51	
OE3	23.56		10.1		1.41		0.23	
OE3	23.1		9.3		1.46		0.2	
OE3	22.81		10.22		1.11		0.24	
OE3	22.37		4.43		0.86		0.63	
OE3	21.58		10.38		0.76		0.49	
OE3 average	21.74	0.0062	7.29	< 0,0001	1.11	0.0004	0.51	0.0024

Table S4: Accession numbers of the proteins utilized in the bHLH-PAS phylogenetic analysis.

SPECIES	ABBREVIATION	ACCESSION	ACCESSION(Alt)
Amphiprora sp., Strain CCMP467	Amph	CAMPEP_0168730192	
Asterionellopsis glacialis, Strain CCMP134	Agla2	CAMPEP_0195290872	
Asterionellopsis glacialis, Strain CCMP1581	Agla3	CAMPEP_0197142484	
Astrosyne radiata, Strain 13vi08-1A	Arad1	CAMPEP_0116831938	
Astrosyne radiata, Strain 13vi08-1A	Arad2	CAMPEP_0116837632	
Attheya septentrionalis, Strain CCMP2084	Asep	CAMPEP_0198303966	
Capsaspora owczarzaki ATCC 30864	Cowc1	XP_004345696	
Capsaspora owczarzaki ATCC 30864	Cowc2	XP_004343694	
Chaetoceros debilis, Strain MM31A-1	Cdeb	CAMPEP_0194099558	
Chaetoceros dichaeta, Strain CCMP1751	Cdic	CAMPEP_0198277646	
Chaetoceros neogracile, Strain CCMP1317	Cneo2	CAMPEP_0195415676	
Chaetoceros neogracile, Strain CCMP1317	Cneo3	CAMPEP_0195453836	
Chaetoceros sp., Strain GSL56	Chae	CAMPEP_0176495412	
Corethron hystrix, Strain 308	Chys	CAMPEP_0113330172	
Corethron pennatum, Strain L29A3	Cpen	CAMPEP_0194280324	
Cyclophora tenuis, Strain ECT3854	Cten1	CAMPEP_0116540656	
Cyclophora tenuis, Strain ECT3854	Cten2	CAMPEP_0116579710	
Cyclotella meneghiniana, Strain CCMP 338	Cmen	CAMPEP_0172279412	
Cylindrotheca closterium	Cclo	CAMPEP_0113624952	
Dactyliosolen fragilissimus	Dfra	CAMPEP_0184871870	
Detonula confervacea, Strain CCMP 353	Dcon	CAMPEP_0172306268	
Ditylum brightwellii, Strain Pop2 (SS10)	Dbri	CAMPEP_0181012646	
Drosophila melanogaster	dmClock	AAC62234	FBpp0099478
Drosophila melanogaster	dmCycle	NP_524168	FBpp0074693
Drosophila melanogaster	dmSim	AAC64519	FBpp0082178
Drosophila melanogaster	dmTango	NP_731308	FBpp0081483
Drosophila melanogaster	dmTrh	AAA96754	FBpp0293065
Durinskia baltica, Strain CSIRO CS-38	Dbal	CAMPEP_0170381008	
Ectocarpus siliculosus	Esil1	Ec-02_004780 PAS domain (681) ;mRNA; f:5082087-5086119	
Eucampia antarctica, Strain CCMP1452	Eant	CAMPEP_0197830682	
Extubocellulus spinifer, Strain CCMP396	Espi1	CAMPEP_0178587872	
Extubocellulus spinifer, Strain CCMP396	Espi2	CAMPEP_0178723458	
Fragilariopsis kerguelensis, Strain L26-C5	Fkue1	CAMPEP_0170867208	
Fragilariopsis kerguelensis, Strain L26-C5	Fkue2	CAMPEP_0170907188	
Fragylariopsis cylindrus	FcbHLH1a	jgi|Fracy1|204663	
Fragylariopsis cylindrus	FcbHLH4	jgi|Fracy1|241747	
Fragylariopsis cylindrus	FcbHLH7	jgi|Fracy1|172104	
Galdieria sulphuraria	Gsul	XP_005709404	
Glenodinium foliaceum, Strain CCAP 1116/3	Gfol1	CAMPEP_0167841300	
Grammatophora oceanica, Strain CCMP 410	Goce	CAMPEP_0194036250	

Guillardia theta CCMP2712	Gthe1	XP_005835918	
Homo sapiens	hsArnt	AAA51777	
Homo sapiens	hsbMal1	NP_1284651	
Homo sapiens	hsClock	AAB83969	
Homo sapiens	hsNpas1	AAH39016	
Homo sapiens	hsSim2	NP_5060	
Kryptoperidinium foliaceum, Strain CCMP 1326	Kfol1	CAMPEP_0176099000	
Leptocylindrus danicus var. danicus, Strain B650	Ldan1	CAMPEP_0116039394	
Leptocylindrus danicus var. danicus, Strain B651	Ldan2	CAMPEP_0116053596	
Leptocylindrus danicus, Strain CCMP1856	Ldan3	CAMPEP_0196809694	
Licmophora paradoxa, Strain CCMP2313	Lpar	CAMPEP_0202478474	
Minutocellus polymorphus, Strain RCC2270	Mpol	CAMPEP_0185804732	
Monosiga brevicollis	Mbre2	jgi|Monbr1|26507|	
Mus musculus	mmArnt	AAA56717	
Mus musculus	mmbMal1b	BAD26600	
Mus musculus	mmbMal2	ABC50103	
Mus musculus	mmClock	AAC53200	
Mus musculus	mmNpas1	NP_32744	
Mus musculus	mmSim2	AAA91202	
Nannochloropsis gaditana CCMP526	Ngad_2	Naga_100016g14	
Nannochloropsis gaditana CCMP526	Ngad_3	Naga_100165g4	
Nannochloropsis oceanica CCMP1779	Noce	NannoCCMP1779_9983-mRNA-1	
Nannochloropsis oceanica CCMP1779	Noce_2	NannoCCMP1779_1600-mRNA-1	
Nitzschia punctata, Strain CCMP561	Npun	CAMPEP_0178827522	
Nitzschia sp.	Nitz	CAMPEP_0113465330	
Phaeodactylum tricornutum	PtbHLH1a	jgi|Phatr2|44962	Phatr3_J44962
Phaeodactylum tricornutum	PtbHLH1b	jgi|Phatr2|44963	Phatr3_J44963
Phaeodactylum tricornutum	PtbHLH2	jgi|Phatr2|54435	Phatr3_J54435
Proboscia alata, Strain PI-D3	Pala	CAMPEP_0194393728	
Pseudo-nitzschia arenysensis, Strain B593	Pare	CAMPEP_0116139930	
Pseudo-nitzschia australis, Strain 10249 10 AB	Paus1	CAMPEP_0168282354	
Pseudo-nitzschia australis, Strain 10249 10 AB	Paus2	CAMPEP_0168310394	
Pseudo-nitzschia delicatissima, Strain B596	Pdel1	CAMPEP_0116091770	
Pseudo-nitzschia delicatissima, Strain B596	Pdel2	CAMPEP_0116094064	
Pseudo-nitzschia fraudulenta, Strain WWA7	Pfra1	CAMPEP_0201229664	
Pseudo-nitzschia fraudulenta, Strain WWA7	Pfra2	CAMPEP_0201232896	
Pseudo-nitzschia heimii, Strain UNC1101	Phei1	CAMPEP_0197189528	
Pseudo-nitzschia heimii, Strain UNC1101	Phei2	CAMPEP_0197199168	
Pseudo-nitzschia multiseries	PmbHLH1a	jgi|Psemu1|26622	
Pseudo-nitzschia multiseries	PmbHLH7	jgi|Psemu1|228145	
Pseudo-nitzschia pungens, Strain cf. pungens	Ppun	CAMPEP_0172413298	
Rhizosolenia setigera, Strain CCMP 1694	Rset	CAMPEP_0178942232	
Skeletonema costatum, Strain 1716	Scos1	CAMPEP_0113408658	

Skeletonema dohrnii, Strain SkelB	Sdoh	CAMPEP_0195221452	
Skeletonema japonicum, Strain CCMP2506	Sjap	CAMPEP_0201725346	
Skeletonema marinoi, Strain FE7	Smar1	CAMPEP_0180846198	
Skeletonema marinoi, Strain UNC1201	Smar2	CAMPEP_0197231700	
Skeletonema menzelii, Strain CCMP793	Smen	CAMPEP_0183679140	
Stauroneis constricta, Strain CCMP1120	Scon1	CAMPEP_0119548954	
Stauroneis constricta, Strain CCMP1120	Scon2	CAMPEP_0119572288	
Staurosira complex sp., Strain CCMP2646	Stau	CAMPEP_0202487246	
Synedropsis recta cf, Strain CCMP1620	Srec1	CAMPEP_0119009808	
Synedropsis recta cf, Strain CCMP1620	Srec2	CAMPEP_0119029558	
Thalassionema frauenfeldii, Strain CCMP 1798	Tfra1	CAMPEP_0178899126	
Thalassionema frauenfeldii, Strain CCMP 1798	Tfra2	CAMPEP_0178923098	
Thalassionema nitzschioides, Strain L26-B	Tnit1	CAMPEP_0194218124	
Thalassionema nitzschioides, Strain L26-B	Tnit2	CAMPEP_0194240022	
Thalassiosira antarctica, Strain CCMP982	Tant	CAMPEP_0202006238	
Thalassiosira gravida, Strain GMp14c1	Tgra	CAMPEP_0201684800	
Thalassiosira miniscula, Strain CCMP1093	Tmin	CAMPEP_0183747574	
Thalassiosira oceanica	Toce2	EJK65393	
Thalassiosira pseudonana	TpbHLH1	jgi|Thaps3|24007	
Thalassiosira pseudonana	TpbHLH2	jgi|Thaps3|20899	
Thalassiosira pseudonana	TpbHLH7	jgi|Thaps3|23208	
Thalassiosira sp., Strain FW	Tfw	CAMPEP_0172354094	
Thalassiosira weissflogii, Strain CCMP1010	Twei	CAMPEP_0203515806	
Thalassiothrix antarctica, Strain L6-D1	Txnt	CAMPEP_0194143228	
Tiarina fusus, Strain LIS	Tfus1	CAMPEP_0117003500	
Tiarina fusus, Strain LIS	Tfus3	CAMPEP_0117046192	

Table S5: List of the oligonucleotides used in this work.

Gene	Phatr3 Accession	Oligo name	Sequence	Type
bHLH1a	Phatr3_J44962	bHLH1a-endogenous-QFw	TTATGTCTTTCGGCGACGGG	QPCR
		bHLH1a-endogenous-QRv	AGCAACGAATGCATGCAAGG	
		bHLH1a-total-QFw	ATTCTTGGTCCCACCCGGTA	QPCR
		bHLH1a-total-QRv	ACGCCACATTGAAAAACCGAG	
		Pt-bHLH1a-DraI-Fw	GATTTTAAAATGAATAAGCCAGGACAGCG	Full lenght cloning
		Pt-bHLH1a-XhoI-Rv	TTGCTCGAGCACAGCTTCGCTGCATCGTC	
bHLH1b	Phatr3_J44963	bHLH1b-QFw	TGCGATCTCAACGGCTAATA	QPCR
		bHLH1b-QRv	CGCAAAACGAGGCTAATTTC	
bHLH3	Phatr3_J42586	bHLH3-QFw	CACTCTCATCATGCGGGAAT	QPCR
		bHLH3-QRv	GCGCGTTGTCTTCCTCTATC	
bZIP7	Phatr3_J48800	bZIP7-QFw	CCTTATTGATATTCAAGATTCCAAGG	QPCR
		bZIP7-QRv	GTTTCGGAACCTGCATAGGA	
bZIP5	Phatr3_J45142	bZIP5-QFw	ACCGGGTACAAAGAAGTCGC	QPCR
		bZIP5-QRv	GACCCTCCAAGCTCTGCATT	
CYCH1	Phatr3_J36892	CYCH1-QFw	ATACACGACGAGCGGATAC	QPCR
		CYCH1-QRv	AACAAGACGCCGTAAATCG	
CYCB1	Phatr3_J46095	CYCB1-QFw	TCCTGGTCCGCTACTTGAAAG	QPCR
		CYCB1-QRv	GCTGGCTGGGAAGATAACGC	
HSF1d	Phatr3_J44750	HSF1d -QFw	TGCTCCATCAAGATACCACCAAT	QPCR
		HSF1d -QRv	GACGACACCCGAAGCTTGTT	
HSF1g	Phatr3_J42514	HSF1g-QFw	AGTTCCCTGTCAGACTCAGC	QPCR
		HSF1g -QRv	ACACTTTCGCCTCTACTGTCA	
HSF3.3a	Phatr3_J45393	HSF3.3a-QFw	CCTTCGAATTCCACTGCACC	QPCR
		HSF3.3a-QRv	CGTAGCCTTCCATCCGTAGT	
HSF4.7b	Phatr3_J49596	HSF4.7b-QFw	GACGACACCCGAAGCTTGTT	QPCR
		HSF4.7b-QRv	ACG AAGCGATCTTGGACAGT	
Tbp	Phatr3_J10199	Tbp-QFw	ACCGGAGTCAAGAGCACACAC	QPCR
		Tbp-QRv	CGGAATGCGCGTATACCAGT	
Rps	Phatr3_J10847	Rps-QFw	CGAAGTCAACCAGGAAACCAA	QPCR
		Rps-QRv	GTGCAAGAGACCGGACATACC	

References

1. Guillard RRL (1975) Culture of Phytoplankton for Feeding Marine Invertebrates. In *Culture of Marine Invertebrate Animals*. Smith DR and Chanley MH (Springer US).
2. Zielinski T, Moore AM, Troup E, Halliday KJ, Millar AJ (2014) Strengths and limitations of period estimation methods for circadian data. *PLoS One* 9(5):e96462.
3. Plautz JD, et al. (1997) Quantitative analysis of Drosophila period gene transcription in living animals. *J Biol Rhythms* 12:204–217.
4. Doyle MR, et al. (2002) The ELF4 gene controls circadian rhythms and flowering time in *Arabidopsis thaliana*. *Nature* 419(6902):74-77.
5. Geiss GK, et al. (2008) Direct multiplexed measurement of gene expression with color-coded probe pairs. *Nature biotechnology* 26(3):317-325.
6. Annunziata R. et al. (2019) Data from "bHLH-PAS protein RITMO1 regulates diel biological rhythms in the marine diatom *Phaeodactylum tricornutum*". Gene Expression Omnibus. Available at https://www.ncbi.nlm.nih.gov/geo/ (Series GSE112268). Deposited March 23, 2018.
7. Coesel S, et al. (2009) Diatom *Pt*CPF1 is a new cryptochrome/photolyase family member with DNA repair and transcription regulation activity. *EMBO Rep* 10(6):655-661.
8. Bhasin M, Raghava GP (2004) ESLpred: SVM-based method for subcellular localization of eukaryotic proteins using dipeptide composition and PSI-BLAST. *Nucleic Acids Res* 32(Web Server issue):W414-419.
9. Almagro Armenteros JJ, Sonderby CK, Sonderby SK, Nielsen H, Winther O (2017) DeepLoc: prediction of protein subcellular localization using deep learning. *Bioinformatics* 33(21):3387-3395.
10. Siaut M, et al. (2007) Molecular toolbox for studying diatom biology in *Phaeodactylum tricornutum*. *Gene* 406(1-2):23-35.
11. Falciatore A, Casotti R, Leblanc C, Abrescia C, Bowler C (1999) Transformation of Nonselectable Reporter Genes in Marine Diatoms. *Mar Biotechnol* (NY) 1(3):239-251.
12. Chauton MS, Winge P, Brembu T, Vadstein O, Bones AM (2013) Gene regulation of carbon fixation, storage, and utilization in the diatom *Phaeodactylum tricornutum* acclimated to light/dark cycles. *Plant physiology* 161(2):1034-1048.
13. Saeed AI, et al. (2003) TM4: a free, open-source system for microarray data management and analysis. *Biotechniques* 34(2):374-378.
14. Keeling PJ, et al. (2014) The Marine Microbial Eukaryote Transcriptome Sequencing Project (MMETSP): illuminating the functional diversity of eukaryotic life in the oceans through transcriptome sequencing. *PLoS Biol* 12(6):e1001889.
15. Katoh K, Standley DM (2013) MAFFT multiple sequence alignment software version 7: improvements in performance and usability. *Mol Biol Evol* 30(4):772-780.
16. Pires N, Dolan L (2010) Origin and diversification of basic-helix-loop-helix proteins in plants. Mol Biol Evol 27(4):862-874.
17. Kumar S, Stecher G, Tamura K (2016) MEGA7: Molecular Evolutionary Genetics Analysis Version 7.0 for Bigger Datasets. *Mol Biol Evol* 33(7):1870-1874.
18. Darriba D, Taboada GL, Doallo R, Posada D (2011) ProtTest 3: fast selection of best-fit models of protein evolution. *Bioinformatics* 27(8):1164-1165.
19. Miller MA, et al. (2015) A RESTful API for Access to Phylogenetic Tools via the CIPRES Science Gateway. *Evol Bioinform Online* 11:43-48.
20. Agier N, Fischer G (2016) A Versatile Procedure to Generate Genome-Wide Spatiotemporal Program of Replication in Yeast Species. *Methods Mol Biol* 1361:247-264.

21. Smith SR, et al. (2017) Transcriptional Orchestration of the Global Cellular Response of a Model Pennate Diatom to Diel Light Cycling under Iron Limitation. *PLoS Genet* 13(3):e1006688.